Plenary lectures

Stability of Rock Structures, Hatzor (ed)
© 2002 Swets & Zeitlinger, Lisse, ISBN 90 5809 519 3

Realistic dynamic analysis of jointed rock slopes using DDA

Y.H. Hatzor, A.A. Arzi, and M. Tsesarsky
Department of Geological and Environmental Sciences, Ben Gurion University of the Negev, Beer–Sheva, Israel

ABSTRACT: A fully dynamic, two dimensional, stability analysis of a highly discontinuous rock slope is demonstrated in this paper using DDA. The analytically determined failure modes of critical keyblocks are clearly predicted by DDA. However, application of a fully dynamic analysis with no damping results in unrealistically large displacements that cannot be confirmed by field studies. With introduction of dynamic damping the calculated results can be made to match historic evidence. Our study shows that introduction of at least 5% dynamic damping is necessary to predict realistically the earthquake damage in a highly discontinuous rock slope with about 400 individual blocks. The introduction of dynamic damping is necessary to account for 2D limitations as well as for various energy loss mechanisms, which are not modeled in DDA.

1 INTRODUCTION

Mount Masada is a table mountain, having a comparatively flat summit surrounded by steep slopes, rising about 480 meters above the nearby Dead Sea. The uppermost tens of meters of the slopes consist of nearly vertical cliffs.

About two thousand years ago, King Herod fortified the mountain and built a major palace based on three natural rock terraces at the northern tip of the summit (Figure 1).

Mount Masada was the site of heroic Jewish resistance against the Romans. It is a national historic monument. The Israel Nature and Parks Authority commissioned this study of the stability of the upper rock terrace of Herod's Palace under earthquake loading, as part of its preservation work.

We carried out the stability evaluation using a fully dynamic version of DDA, with inputs based on a comprehensive field and laboratory study.

Figure 1. A photo of the North Face of Masada showing the upper terrace of King Herod's Palace.

2 GEOLOGICAL – SEISMOLOGICAL SETTING

The upper portion of Mount Masada consists of essentially bare hard rock. The rock is mainly bedded limestone and dolomite, with near vertical jointing. Structurally, the entire mountain is an uplifted block within the band of faults which forms the western boundary of the Dead Sea Rift.

The Dead Sea Rift is a seismically active transform (Garfunkel et al., 1981; Garfunkel and Ben-Avraham,

1996). According to the Israel building code – Israel Standard 413, based on research by the Geophysical Institute of Israel Seismology Division, under the direction of Dr. A. Shapira, the Dead Sea region has been classified as a region in which an earthquake-induced peak ground acceleration. (PGA) exceeding 0.2 *g* at the deep bedrock level is expected with a 10% probability within any 50 year window. This is analogous to a 475 year average recurrence interval for such acceleration. In this paper we repeatedly refer to PGA for simplicity, which is adequate in the present context, although PGA is not generally the best measure of destructive potential (Shapira, 1983; Shapira and van Eck, 1993).

Inspection of the historic earthquake record (Ben-Menahem, 1979; Turcotte and Arieh, 1988; Amiran et al., 1994) suggests that the strongest shaking events which have actually affected Mount Masada within the past two thousand years were due to about ten identified earthquakes with estimated magnitudes in the range of 6.0 ± 0.4 and focal distances probably in the order of several kilometers to a few tens of kilometers from the site. With these parameters, it is highly likely that some of these earthquakes have caused at Mount Masada bedrock PGA's reaching and even exceeding 0.2 *g*, in general agreement with predictions for a 2000 year period based on the aforementioned building code assumptions.

One of the most notable historic earthquakes in this region occurred probably in the year 362 or 363, with a magnitude estimated at 6.4 (Ben-Menahem, 1979) or even 7.0 (Turcotte and Arieh, 1988). Reported effects included a tsunami in the Dead Sea and destruction in cities tens of kilometers from the Dead Sea both east and west. This is probably the earthquake identified by archeologists as "the great earthquake which destroyed most of the walls on Masada sometime during the second to the fourth centuries" (Netzer, 1991).

The most recent of the major historic earthquakes near Mount Masada occurred on July 11th, 1927. This earthquake was recorded by tens of seismographs, yielding a magnitude determination of 6.2 and an epicenter location 30 ± 10 km north of Masada. It also caused a tsunami in the Dead Sea and destruction in cities tens of kilometers away (Shapira et al., 1993)

3 OBSERVED HISTORICAL STABILITY

The fortifications built by King Herod on Mount Masada about two thousands years ago (Netzer, 1991) included a casemate wall surrounding the relatively flat top of the mountain. Clearly, because of its defensive function, the outer face of this wall was built so as to continue upward the face of the natural cliff, as much as possible.

The outer wall was therefore founded typically on the flat top within several decimeters from its rim. Locally it was even founded slightly beyond the rim, on a somewhat lower edge of rock. On the aforementioned three palace terraces, jutting at the northern tip of the mountain top, construction was again carried out up to the rim and beyond in order to achieve architectural effects and utilize fully the limited space.

Thus, the remaining foundations effectively serve to delineate the position of the natural rim of the flat mountain top and associated northern terraces about 2000 years ago. Missing portions along such foundation lines indicate locations in which the rim has most probably receded due to rockfalls, unless the portions are missing due to other obvious reasons such as local erosion of the flat top by water or an apparent location of the foundation on fill beyond the rim.

Our inspection of the entire rim of the top of Masada, aided by Hebrew University archeologist Guy Stiebel, reveals that over almost the entire length of the casemate wall, which is about 1400 m, the rock rim has not receded during the past two thousand years more than a few decimeters, if at all. Only over a cumulative total of less than 40 m, i.e. about 3% of the wall length, there are indications of rockfalls involving rim recessions exceeding 1.5 m, but not exceeding 4.0 m. Since the height of the nearly-vertical cliffs below the rim is in the order of tens of meters, these observations attest to remarkable overall stability in the face of the recurring earthquakes.

On King Herod's palace terraces there has been apparent widespread destruction, mostly of walls and fills which were somehow founded on the steep slopes. However, in the natural cliffs themselves there are few indications of rockfalls involving rim recessions of more than a few decimeters. Remarkably, most of the high retaining walls surrounding the middle and lower terraces are still standing, attesting to the stability of the rock behind them. In the upper terrace, on which this study is focused, there appears to be only one rockfall with depth exceeding several decimeters. It is a local rockfall near the top of the 22 m cliff, in the northeast, causing a rim recession of about 2.0 m. It is notable that this particular section of the terrace cliff was substantially modified by the palace builders, perhaps de-stabilizing the preexisting natural cliff.

We have also inspected rare aerial photographs of Mount Masada dated December 29th 1924, i.e. predating the 1927 earthquake. Our comparison with recent aerial photographs would have been capable of detecting rim recessions exceeding about one meter, if any had occurred in the northern part of the mountain. None were found, suggesting that the 1927 earthquake did not cause any significant rockfalls there (the southern part was less clear in the old photographs).

The information presented above essentially constitutes results of a rare rock-mechanics field-scale "experiment". Two thousand years ago the Masada cliff top was marked by construction. The mountain was later shaken by several major earthquakes, with

deep bedrock accelerations certainly exceeding 0.1 g and probably even exceeding 0.2 g. Due to the topography affect, motions at the top are substantially amplified at frequencies about 1.3 Hz (Zaslavsky et al., 2002).

Observations at the present stage of the "experiment" show that all the cliffs surrounding the top of Mount Masada essentially withstood the shaking, with some relatively minor rockfalls at the top of the cliffs.

The above is a substantial result of a full-scale "experiment" on the real rock structure. Therefore, a fundamental test of any model of this structure is that it must essentially duplicate the above "experiment". As shown in the sequel, we subjected our DDA model to this test, obtaining instructive results.

4 MECHANICAL BEHAVIOR OF THE ROCK AT MASADA

4.1 *Rock mass structure*

Herod's Palace, also known as the North Palace, is built on three terraces at the north face of Masada. The rock mass structure at the foundations consists of two orthogonal, sub vertical, joint sets striking roughly parallel and normal to the NE trending axis of the mountain, and a set of well developed bedding planes gently dipping to the north (Table 1). The joints are persistent, with mean length of 2.7 m. The bedding planes, designated here as J_1, dip gently to the north with mean spacing of 60 cm. The two joint sets, J_2 and J_3, are closely spaced with mean spacing of 14 cm and 17 cm respectively (Figure 2).

4.2 *Physical properties*

The rock mass consists of bedded dolomites with local karstic voids between beds. The bulk porosity of intact samples ranges between 3% – 12% and the dry unit weight is 25 kN/m^3. The bedding planes are generally clean and tight.

4.3 *Strength and elasticity of intact rock*

The elastic behavior of the rock was studied using a stiff, hydraulic, closed-loop servo controlled load frame with maximum axial force of 1.4 MN, and stiffness of $5 * 10^9$ N/m (Terra-Tek model FX-S-33090). Testing procedures are described by Hatzor and Palchik, 1997, 1998) and Palchik and Hatzor (2002). Tests were performed at a constant strain rate of $5 * 10^{-6}$ s^{-1}. In Figure 3 the result of a load – unload loop of uniaxial compression performed on a solid cylinder from the dolomite at Masada is shown. This result indicates that the uniaxial compressive strength of the tested dolomite sample is greater than 315 MPa, that the elastic modulus is 43 GPa, and that Poisson's ratio is 0.18 (radial strains are not shown). These data

Table 1. Discontinuity data for the foundations of King Herod's Palace – Masada.

Set #	Type	Dip	s m	C MPa	$\phi°$
1	Bedding	5/N	0.60	0	41°
2	Joints	80/ESE	0.14	0	41°
3	Joints	80/NNE	0.17	0	41°

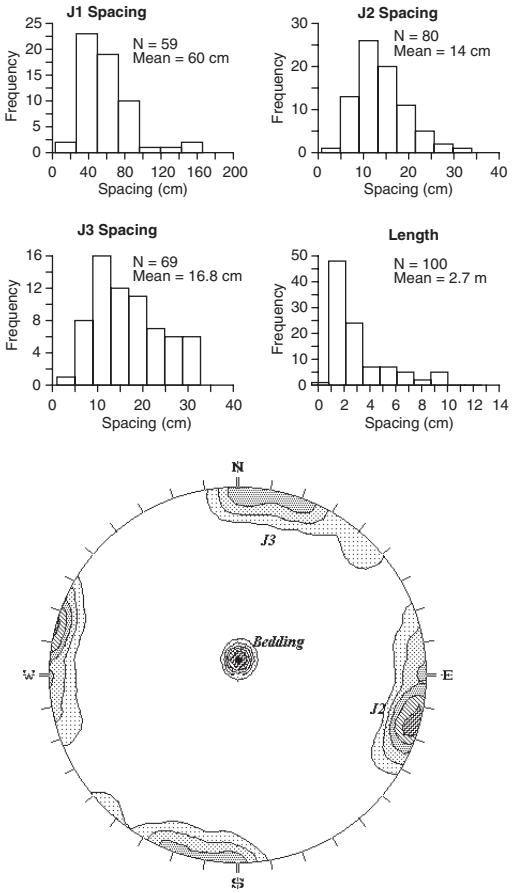

Figure 2. Discontinuity length, spacing, and orientation distribution at the foundations of King Herod's Palace, Masada. Upper Hemisphere projection of poles.

fall within the range of strength and elasticity values determined experimentally for other dolomites in Israel (Hatzor and Palchik, 1997, 1998; Palchik and Hatzor, 2002).

4.4 *Residual shear strength of discontinuities*

The residual friction angle of joints was determined using tilt tests performed on saw-cut and ground surfaces of dolomite, assuming the joint planes are

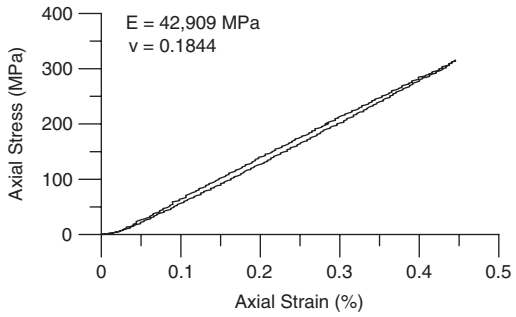

Figure 3. Result of a load – unload cycle under uniaxial compression performed on an NX size solid cylinder of the dolomite in Masada.

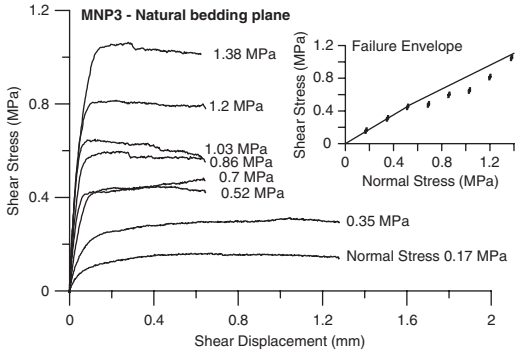

Figure 4. Shear stress vs. shear displacement for a natural bedding plane sample from the foundations of Herod's Palace in Masada.

clean and tight. 20 tilt tests performed on saw-cut and ground surfaces provided a mean friction angle of 28° and 23° respectively. The 5° difference is attributed to roughness resulting from saw-cutting.

4.5 *Shear strength of filled bedding planes*

The shear strength of filled bedding planes was estimated using a segment triaxial test performed on a right cylinder containing an inclined saw cut plane at 55° to the axis of the cylinder, filled with crushed dolomite. Seven different segments were performed, with confining pressure values ranging between 2.2 and 16.2 MPa. A linear Coulomb – Mohr failure criterion was found, with zero cohesion and a residual friction angle of 22.7°. The test procedures and results are discussed by Hatzor (in press). The similarity between the result of tilt tests on ground surfaces (23°) and the segment triaxial test on a filled saw-cut plane (22.7°) suggests that during shear the infilling material crushed all remaining asperities in the saw-cut sample resulting in a failure envelope representing residual conditions. The residual friction angle value of 23° may therefore be applicable for very large blocks where some initial shear displacements have already taken place due to historic cycles of seismic loading (see Hatzor, in press). However, for dynamic analysis of smaller blocks with high static factor of safety the strengthening effect of initial asperities ought to be considered.

4.6 *Shear strength of rough bedding planes*

The shear strength of rough bedding planes was determined using real bedding plane samples from the foundations of the North Palace. The upper and lower sides of the mating planes were kept in contact with no disturbance and were transported to the lab at natural water content. The two samples were cast inside two $200\,\text{mm} * 200\,\text{mm} * 150\,\text{mm}$ shear boxes while the mating surfaces were kept intact. The gap between the rock and the box frame was filled with Portland cement.

Direct shear tests were performed using a hydraulic, close loop servo-controlled, direct shear system with normal force capacity of 1000 kN and horizontal force capacity of 300 kN (Product of TerraTek Systems Inc.). The stiffness of the normal and shear load frames is 7.0 and 3.5 MN/m respectively. Normal and horizontal displacement during shear were measured using four and two 50 mm LVDT's with 0.25% linearity full scale. Axial load was measured using a 1000 kN capacity load cell with 0.5% linearity full scale. Shear load was measured using a 300 kN load cell with 0.5% linearity full scale.

The direct shear tests were performed for two samples (MNP2, MNP3) under constant normal stress and shear displacement rate of 1mil/sec (0.025 mm/sec). In Figure 4 shear stress vs. shear displacement is shown for sample MNP-3 that was loaded, unloaded, and reloaded in eight cycles of increasing normal stress from 0.17 MPa to 1.38 MPa. In each cycle the sample was sheared forward, in the first cycle a distance of 1.3 mm, and then additional 0.5 mm of forward shear displacement in each consecutive segment. Plotting the peak shear stress vs. normal load for the two segment tests (Figure 5) reveals a bilinear failure envelope with the following failure criterion:

$$0 < \sigma_n < 0.5\,MPa : \tau = 0.88\sigma_n \; (R^2 = 0.999)$$

$$0.5 < \sigma_n \leq 12\,MPa : \tau = 0.083 + 0.71\sigma_n (R^2 = 0.998)$$

These results indicate that for low normal load (up to 0.5 MPa) the peak friction angle for the bedding planes at Masada is 41.3°. For higher normal loads the peak friction angle is 35.3°. The residual friction angle may be taken from the triaxial tests of the filled discontinuities as 23°. The maximum height of the terrace at the North Palace is 25 m and therefore the normal stress acting on bedding planes at the North

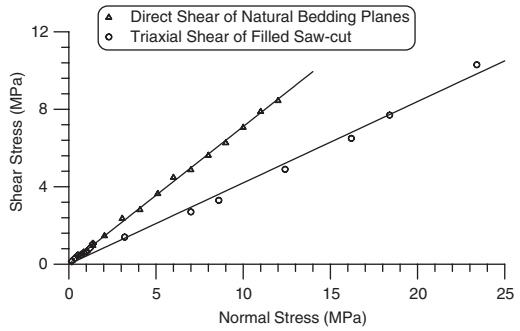

Figure 5. Failure envelope for rough bedding planes – direct shear tests.

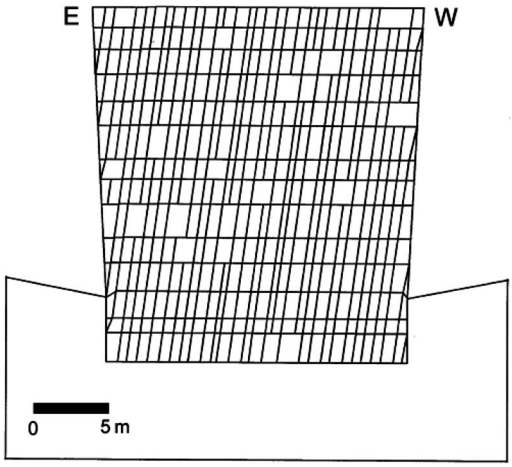

Figure 6. A synthetic joint trace map of the upper rock terrace of Herod's Palace in Masada using the statistical joint trace generation code (DL) of Shi (1993).

Palace cannot be greater than 682 kPa. Therefore, in light of the experimental results, the low normal load criterion should be used for dynamic analysis.

5 MESH GENERATION METHODS AND EXPECTED FAILURE MODES

5.1 *Synthetic joint trace generation*

Two principal joint sets and a systematic set of bedding planes comprise the structure of the foundations of Herod's Palace (Figure 2). An E-W cross section of the upper terrace is shown in Figure 6, computed using the statistical joint trace generation code (DL) of Shi (1993). It can be seen intuitively that while the East face of the rock terrace is prone to sliding of wedges, the West face is more likely to fail by toppling of

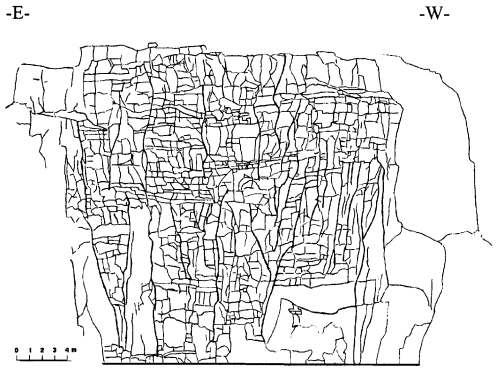

Figure 7. A photogeological trace map of the northern face of Herod's Palace upper terrace.

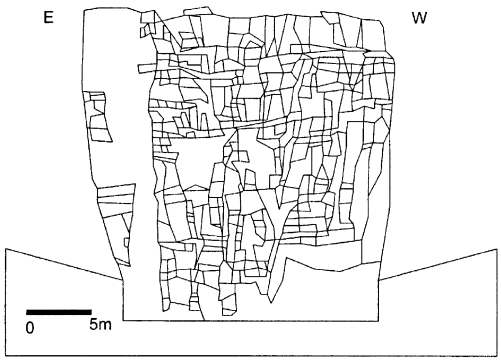

Figure 8. A deterministic joint trace map of the terrace prepared using the photogeological map (Figure 7) and the block cutting algorithm (DC) of Shi (1993).

individual blocks. Kinematic, mode, and removability analyses confirm these intuitive expectations.

5.2 *Deterministic joint trace generation*

While it is quite convenient to use mean joint set attitudes and spacings in order to generate statistically a synthetic mesh, the resulting mesh is quite unrealistic and bears little resemblance to the actual slope. The contact between blocks obtained this way is unrealistically planar, thus interlocking between blocks is not modeled. Consequently the results of dynamic calculations will be overly conservative.

In order to analyze the dynamic response of the slope realistically a photo-geological trace map of the face was prepared using aerial photographs (Figure 7), and the trace lines were then digitized. Thus, the block-cutting (DC code) algorithm of Shi (1993) could be utilized in order to generate a trace map which represents more closely the reality in the field (Figure 8).

The same failure modes would be anticipated in the deterministic mesh shown in Figure 8. However, the interlocking between blocks within the slope is much higher and therefore the results of the dynamic analysis should be less conservative and more realistic.

6 INPUT MOTION FOR DYNAMIC ANALYSIS

In order to perform a realistic dynamic analysis for the rock slopes at Masada, we prefer modeled input motion representing ground motions for the Dead Sea rift system. In this research we chose to use the recorded time history of the Mw = 7.1. Nuweiba earthquake which occurred in November 1995 in the Gulf of Eilat (Aqaba) with an epicenter near the village of Nuweiba, Egypt. The main shock was recorded at the city of Eilat where the tremor was felt by people, and structural damage was detected in houses and buildings. The city of Eilat is located 91 km north from the Nuweiba earthquake epicenter and 186 km south of Masada, on the northern coast of the gulf of Eilat (Aqaba). Figure 9 shows the vertical and EW components of the accelerogram that were recorded in Eilat. The horizontal Peak Ground Acceleration (PGA) of the Nuweiba record was 0.08 *g*.

The Eilat accelerograph station was on a thick fill of Pleistocene alluvial fan deposits. The recorded accelerogram therefore represents the response of a site situated on deep fill rather than on sound bedrock. However, we regard this as a secondary issue in the present context. As shown in the sequel, we utilized as input both the 0.08 *g* PGA accelerogram as well as the same accelerogram normalized to a 0.18 *g* PGA, so as to explore a range of PGA's. As explained in chapters 2 and 3 above, the Masada cliffs, including Herod's Palace upper terrace, have withstood historic earthquakes in this PGA range with only minor rockfalls.

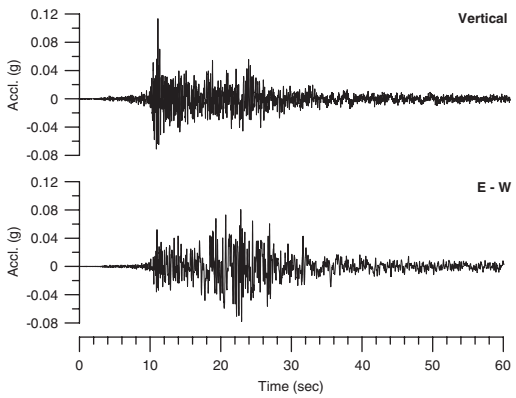

Figure 9. Time history of the Mw = 7.1 Nuweiba earthquake (Nov. 22, 1995) as recorded at the city of Eilat.

7 FULLY DYNAMIC ANALYSIS USING DDA

7.1 *The numerical discontinuous deformation analysis*

The DDA method (Shi, 1993) incorporates dynamics, kinematics, and elastic deformability of geological materials, and models actual displacements of individual blocks in the rock mass using a time-step marching scheme. The formulation is based on minimization of potential energy and uses a "penalty" method to prevent penetration or tension between blocks. Numerical penalties in the form of stiff springs are applied at the contacts to prevent either penetration or tension between blocks. Since tension or penetration at the contacts will result in expansion or contraction of the springs, a process that requires energy, the minimum energy solution is one with no tension or penetration. When the system converges to an equilibrium state however, there are inevitable penetration energies at each contact, which balance the contact forces. Thus, the energy of the penetration (the deformation of the springs) can be used to calculate the normal and shear contact forces.

Shear displacement along boundaries is modeled in DDA using the Coulomb-Mohr failure criterion. The fixed boundaries are implemented using the same penalty method formulation: stiff springs are applied at the fixed points. Since displacement of the fixed points requires great energy, the minimum energy solution will not permit fixed-point displacement. The blocks are simply deformable: stresses and strains within a block are constant across the whole region of the block.

In this research a new C/PC version of DDA, recently developed by Shi (1999), is used. In this new version earthquake acceleration can be input directly in every time step. A necessary condition for direct input of earthquake acceleration is that the numerical computation has no artificial damping, because damping may reduce the earthquake dynamic energy and the damage may thus be underestimated (Shi, 1999). In DDA the solution of the equilibrium equations is performed without damping (Shi, 1999) for the purpose of a fully dynamic analysis in jointed rock masses. As we shall see below however, application of dynamic DDA with no damping returns unrealistically high displacements and is therefore overly conservative.

7.2 *Validation of dynamic displacement prediction by DDA using analytical solutions*

Hatzor and Feintuch (2001) demonstrated the validity of DDA results for fully dynamic analysis of a single block on an incline subjected to dynamic loading. First the dynamic solution for a single block on an incline subjected to gravitational load (constant acceleration), a case which was investigated originally by MacLaughlin (1997), was repeated using the new

dynamic code (Shi, 1999). For a slope inclination of 22.6°, four dynamic displacement tests were performed for interface friction angle values of 5°, 10°, 15°, and 20°. The agreement between the analytical and DDA solution was within 1–2%. Next, Hatzor and Feintuch investigated three different sinusoidal functions of increasing complexity for the dynamic load input function, and checked the agreement between DDA and the derived analytical solutions. A very good agreement between analytical solution and DDA was obtained in all cases, with errors between 5% to 10% (Figure 10). It was found by Hatzor and Feintuch that in order to get a good agreement between DDA and the analytical solution, the maximum size of the time step (g1) had to be properly conditioned. For example, with increasing block velocity the maximum time step size had to be reduced in order to obtain good agreement with the analytical solution. The best method to estimate the proper time step size would be to check the ratio between the assumed maximum displacement per time step (g2) and the actual displacement per time step calculated by DDA. In order to get good agreement between DDA and the analytical solution that ratio should be as close as possible to 1.0. Such an optimization procedure however is only possible for single block cases.

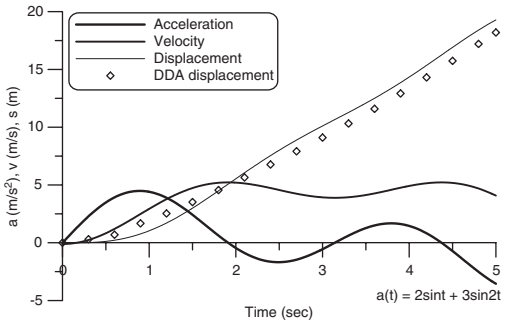

Figure 10. Validation of dynamic DDA using analytical solutions (after Hatzor and Feintuch, 2001).

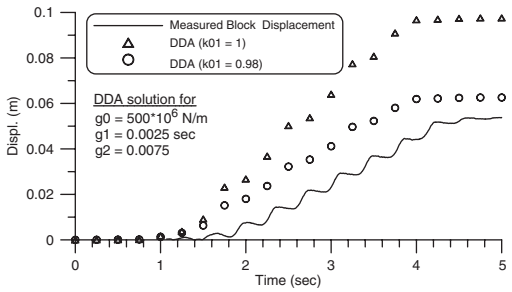

Figure 11. Validation of dynamic DDA using shaking tabel experiments from Berkeley (after Tsesarsky et al., 2002).

7.3 *Validation of dynamic displacement prediction by DDA using shaking table experiments*

The dynamic displacement problem of a block on an incline was studied by Wartman (1999) using shaking table experiments that were performed at the U.C. Berkeley Earthquake Engineering Laboratory. The same tests were repeated numerically by Tsesarsky et al. (2002) using dynamic DDA, and some results are shown in Figure 11 (see complete paper in this volume). The results of Tsesarsky et al. suggest that with zero dynamic damping DDA overestimates the physical displacements by as much as 80%. However, with as little as 2% dynamic damping the results of DDA match the experimental results within 5% accuracy. This result suggests that realistic application of dynamic DDA must introduce some measure of damping in order to account for energy loss mechanisms that are not modeled by DDA, the first of which is energy consumption due to irreversible deformation during block interactions.

The results of Tsesarsky et al. (2002) pertain to a single block on an incline. A multi-block problem was studied by McBride and Scheele (2001), using a slope with a stepped base consisting of 50 blocks that undergo sliding failure under gravitational load. Their conclusion was that as much as 20% dynamic damping was necessary in order to obtain realistic agreement between the physical model and DDA. Perhaps better conditioning of the control parameters would have reduced the required dynamic damping by a significant amount.

8 RESULTS OF DYNAMIC ANALYSIS

8.1 *Numerical details*

In all DDA simulations the complete record was computed for the entire 50 seconds of earthquake duration (see Figure 9). The numerical input parameters used in this work are listed in Tables 2 and 3 (for explanation of each control parameter see Shi, 1993).

DDA computations were performed on a P4-1.5 GHz processor with 128 Mb RAM. To complete the required 25000 time steps (earthquake duration of 50 seconds) approximately 42 hours of processor time were requires, namely a computation rate of approximately 600 time steps per hour. The mesh consists of 344 blocks.

8.2 *Realistic damage prediction by DDA*

In Figure 12 the computed response of the upper terrace is shown with various amounts of dynamic damping. Figure 12A shows the computed damage with zero dynamic damping, namely the initial velocity in every time step is inherited from the previous

Table 2. Numeric Control Parameters.

Total number of time steps:	25,000
Time step size (g1):	0.002
Assumed maximum displacement ratio (g2):	0.0015
Contact spring stiffness (g0):	$5 * 10^6$ kN/m
Factor of over-relaxation:	1.3

Table 3. Material Properties.

Unit weight of rock (γ):	25 kN/m^3
Elastic Modulus (E):	$43 * 10^6$ kN/m^2
Poisson's Ratio (v):	0.184
Friction angle of all discontinuities (ϕ):	41°
Cohesion of all discontinuities (C):	0
Tensile strength of all discontinuities (σ_t):	0

time step. After 50 seconds of shaking, with 0.08 g PGA, the upper terrace seems to disintegrate completely. In light of the historic observations this result is clearly unrealistic.

In Figure 12B the response of the terrace is shown again after 50 seconds of shaking but with 5% dynamic damping, namely the initial velocity of each block at the beginning of a time step is reduced by 5% with respect to its terminal velocity at the end of the previous time step. The model predicts onset of toppling failure at the foot of the west slope and minor sliding deformations at the east slope. The failure modes predicted by the model are similar to the expected modes from both field and analytical studies. The extent of damage in the terrace and the depth of the loosened zone in the west slope are reduced significantly with comparison to the undamped analysis.

The performance of the slope with 10% dynamic damping (Figure 12C) is roughly the same as with 5% dynamic damping and therefore the justification for more than 5% dynamic damping seems questionable.

Assuming that 5% damping is the correct amount necessary to account for energy loss mechanisms ignored by DDA, we studied the response of the terrace slopes to the same accelerogram when normalized to a 0.18 g PGA, which is still within the range of historic earthquakes as discussed in chapters 2,3 and 6 above.

As shown in Figure 13, after 50 seconds of shaking the damage is not much different than that which was modeled for the original time history (Figure 12B). Both Figures 12B and 13 indicate the expected depth of the loosened zone in the slope due to the seismic loading.

We believe that the graphical output in Figure 13 is still very conservative because it does not compensate fully for: a) various real energy dissipation mechanisms, b) reinforcing potential of the third, in slope, dimension.

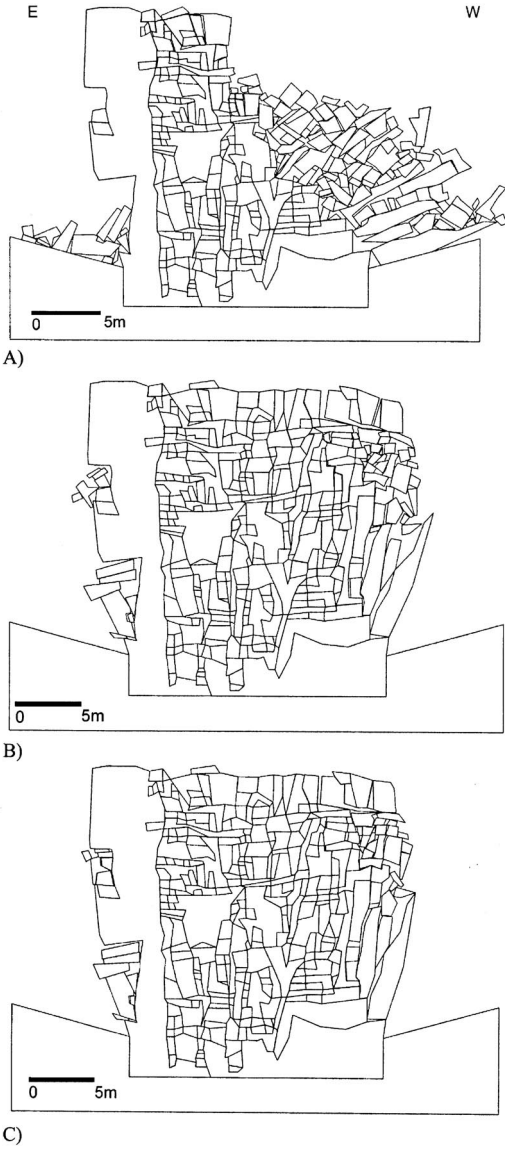

Figure 12. Results of dynamic DDA calculation of the original Nuweiba record (PGA = 0.08 g) after 50 seconds of shaking. A) No dynamic damping in DDA, B) 5% damping, C) 10% damping.

Nevertheless, a graphical result such as the one presented in Figure 13 can be used as an aid for support design. Both the spacing and length of the support elements (anchors or rock bolts) can be dimensioned using the graphical output. The required capacity of the anchors may be estimated using a pseudo-static analysis for a representative block with the peak horizontal acceleration taken for the pseudo-static inertia force.

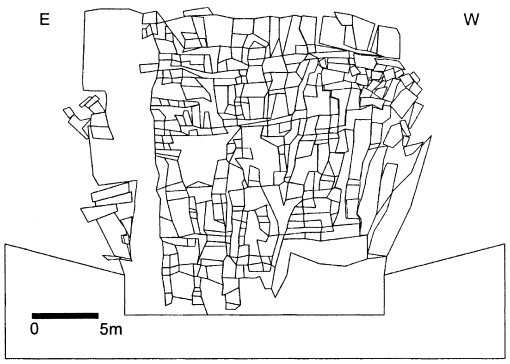

Figure 13. Results of dynamic DDA calculation (with 5% dynamic damping) after 50 seconds of shaking using the Nuweiba record normalized to PGA = 0.18 *g*.

9 SUMMARY AND CONCLUSIONS

In this paper a highly jointed rock slope, which withstood many events of strong seismic ground motions in historic times, is modeled using dynamic DDA. The field observations are compared with the results of the numerical model. The following are tentative conclusions:

- We find that for a realistic calculation of dynamic response the modeled joint trace map (the mesh) must be as similar as possible to the geological reality. We recommend using digitized photogeological trace maps in conjunction with the DC block-cutting algorithm of Shi (1993) in order to generate the realistic mesh, rather than a statistical joint trace generation algorithm such as the DL code of Shi (1993). Such a deterministic approach will capture some block-interlocking mechanisms active in the modeled slope because of dissimilarities in joint attitudes and variations in dip angle along the surface of the discontinuities.
- Previous studies have shown that dynamic DDA with zero dynamic damping will match analytical solutions for a single block on an incline with great accuracy. However, when results of dynamic DDA are compared with shaking table experiments for a single block it is found that at least 2.5% of dynamic damping is necessary for accurate displacement predictions. We believe that the dynamic damping is necessary in order to account for energy loss mechanisms, which are abundant in the physical reality but are ignored by the linear – elastic approach taken by DDA. Also, the dynamic damping may partially compensate for the two dimensional formulation which does not allow modeling the strengthening effect of the third, in slope, dimension.
- Using a real time history from the Dead Sea rift system we modeled the response of the jointed rock slope for which exists a good historic record of stability under recurring strong earthquake shaking. We found that in order to obtain realistic predictions for this multi-block analysis, at least 5% dynamic damping was required.
- Only when proven to be realistic, the graphical output of such an analysis may be used to estimate the depth of the loosening zone following the earthquake, and the spacing, length and capacity of support elements – if required.

ACKNOWLEDGEMENTS

This research was funded by Israel Nature and Parks authority and partially by the Bi-national Science Foundation (BSF) through grant 98-399. The support of the two agencies is hereby acknowledged. A. Shapira and Y. Zaslavsky from the Geophysical Institute of Israel are thanked for the Nuweiba record. Gen-Hua Shi is thanked for making his dynamic DDA code available for this study. Finally, Guy Stiebel is thanked for guiding us on Masada with archeological insights and for providing the 1924 aerial photographs.

REFERENCES

Amiran, D.H.K., Arieh, E. and Turcotte, T. 1994. Earthquakes in Israel and adjacent areas: Macro – seismicity observations since 100 B.C.E. *Israel Explor. J.*, 41, 261–305.

Ben – Menahem, A. 1979. Earthquake Catalog for the Middle East. *Bollettino di Geofisica Teorica e Applicata*, v. XXI, pp. 245–313.

Garfunkel, Z. and Ben-Avraham, Z. 1996. The structure of the Dead Sea basin. In : Dynamics of extensional basins and inversion tectonics. *Tectonophysics*, 266, 155–176.

Garfunkel, Z., Zak, I. and Freund, R., 1981. Active faulting in the Dead Sea Rift. *Tectonophysics*, 80, 1–26.

Hatzor, Y.H. and V. Palchik, 1997. The influence of grain size and porosity on crack initiation stress and critical flaw length in dolomites. *International Journal of Rock Mechanics and Mining Sciences*, Vol. 34, No. 5, pp. 805–816.

Hatzor, Y.H. and Palchik V., 1998. A microstructure-based failure criterion for Aminadav dolomites – Technical Note. *International Journal of Rock Mechanics and Mining Sciences*, Vol. 35, No. 6, pp. 797–805.

Hatzor, Y.H. and Feintuch, A. 2001. The validity of dynamic displacement prediction using DDA. *International Journal of Rock Mechanics and Mining Sciences*, Vol. 38, No. 4, pp. 599–606.

Hatzor, Y.H. in press. Keyblock stability in seismically active rock slopes – the Snake Path cliff – Masada. *Journal of Geotechnical and Geoenvironmental Engineering*, ASCE.

MacLaughlin, M.M. *Discontinuous Deformation Analysis of the kinematics of landslides* 1997. Ph.D. Dissertation, Dept. of Civil and Env. Engrg., University of California, Berkeley.

McBride, A. and Scheele, F. Investigation of discontinuous deformation analysis using physical laboratory models. *Proceedings of ICADD-4, 4th International Conference of Analysis of Discontinuous Deformation* (N. Bicanic Ed) Glasgow, Scotland, UK.

Netzer, E. 1991. Masada III – the Yigael Yadin Excavations 1963–1965. Final Reports – The Buildings Stratigraphy and Architecture. *Israel Exploration Society*, The Hebrew University, Jerusalem, Israel, 665p.

Palchik, V. and Y.H. Hatzor, 2002. Crack damage stress as a composite function of porosity and elastic matrix stiffness in dolomites and limestones. *Engineering Geology*. Vol. 63, pp. 233–245.

Shapira, A. 1983, A probabilistic approach for evaluating earthquake risk with application to the Afro-Eurasian junction, *Tectonophysics*, 95:75–89.

Shapira, A., Avni, R. and Nur, A. 1993. A new estimate for the epicenter of the Jericho earthquake of 11th July 1927. *Israel Journal of Earth Science*, Vol. 42, No. 2, pp. 93–96.

Shapira, A. and van Eck, T. 1993. Synthetic uniform hazard site specific response spectrum, *Natural Hazard*, 8: 201–205

Shi, G.-H. 1993. *Block System Modeling by Discontinuous Deformation Analysis*, Computational Mechanics Publications, Southampton UK, p. 209.

Shi, Gen-Hua, 1999. Application of Discontinuous Deformation Analysis and Manifold Method. *Proceedings of ICADD-3, Third International Conference of Analysis of Discontinuous Deformation* (B. Amadei, Ed) Vail, Colorado, pp. 3–15.

Tsesarsy, M., Hatzor, Y.H. and Sitar, N. 2002. Dynamic block displacement prediction – validation of DDA using analytical solutions and shaking table experiments. *Proceedings of ICADD-5, 5th International Conference of Analysis of Discontinuous Deformation* (Y.H. Hatzor, Ed) Beer-Sheva, Israel. Published by Balkema Rotterdam.

Turcotte, T. and Arieh, E. 1988. Catalog of earthquakes in and around Israel, Appendix 2.5A in: Shivta site Preliminary Safety Analysis Report, Israel Electric Corp. LTD.

Wartman, J. 1999. *Physical model studies of seismically induced deformation in slopes.* Ph.D. thesis, Department of Civil Engineering, University of California, Berkley.

Zaslavsky, Y., Shapira, A. and Arzi, A.A. 2002. Earthquake site response on hard rock – empirical study. *Proceedings of ICADD-5, 5th International Conference on Analysis of Discontinuous Deformation* (Y.H. Hatzor, Ed) Beer Sheva, Israel. Published by Balkema, Rotterdam.